CORNELL UNIVERSITY

Center for Radiophysics and Space Research

ITHACA, N. Y.

[redacted]

CRSR 706

EVAPORATION OF ICE IN PLANETARY ATMOSPHERES: ICE-COVERED RIVERS ON MARS

David Wallace and Carl Sagan

[redacted]

EVAPORATION OF ICE IN PLANETARY ATMOSPHERES:

ICE-COVERED RIVERS ON MARS*

October 1978

By David Wallace and Carl Sagan

Laboratory for Planetary Studies
Cornell University
Ithaca, New York

---

*Presented at the 9th annual meeting of the Division for Planetary Sciences, American Astronomical Society, Boston, Massachusetts, October 29, 1977.

ABSTRACT

The evaporation rate of water ice on the surface of a planet with an atmosphere involves an equilibrium between solar heating and radiative and evaporative cooling of the ice layer. The thickness of the ice is governed principally by the solar flux which penetrates the ice layer and then is conducted back to the surface. These calculations differ from those of Lingenfelter et al. (1968) for putative lunar channels in including the effect of the atmosphere. Evaporation from the surface is governed by two physical phenomena: wind and free convection. In the former case, water vapor diffuses from the surface of the ice through a laminar boundary layer and then is carried away by eddy diffusion above, provided by the wind. The latter case, in the absence of wind, is similar, except that the eddy diffusion is caused by the lower density of water vapor than the martian atmosphere. For mean martian insolations the evaporation rate above the ice is $\sim 10^{-8}$ gm $cm^{-2} s^{-1}$. Thus, even under present martian conditions a flowing channel of liquid water will be covered with ice which evaporates sufficiently slowly that the water below can flow for hundreds of kilometers even with quite modest discharges. Evaporation rates are calculated for a wide range of frictional velocities, atmospheric pressures, and insolations and it seems clear that at least some subset of observed martian channels may have formed as ice-choked rivers. Typical equilibrium thicknesses of such ice covers are $\sim$10 to 30 m; typical surface temperatures are 210 to 235° K. Ice-covered channels or lakes on

Mars today may be of substantial biological interest. Ice is a sufficiently poor conductor of heat that sunlight which penetrates it can cause melting to a depth of several meters or more. Because the obliquity of Mars can vary up to some 35°, the increased polar heating at such times seems able to cause subsurface melting of the ice caps to a depth which corresponds to the observed lamina thickness and may be responsible for the morphology of these polar features.

"Where Alf the Sacred River ran
Through caverns measureless to man
Down to a sunless sea"

----Samuel Taylor Coleridge
Kubla Khan

Martian Channels

In 1962, Lederberg and Sagan argued that Mars, being an outgassed planet with a mean temperature below the freezing point of water, must have substantial reservoirs of permafrost; and that geothermal heating of this permafrost could produce bodies of subsurface liquid water on Mars. The Mariner 6 and 7 fly-by missions of 1969 discovered the existence of "chaotic terrain" on Mars, which has since been generally described as thermokarst, a landform in which the overburden has collapsed because of removal of subsurface water (Sharp et al., 1971; Belcher, Veverka, and Sagan, 1971; Sharp, 1973; Soderblom and Wenner, 1978). A post-Viking discussion of a range of features attributed to permafrost on Mars is made by Carr and Schaber (1977). In 1971, before the Mariner 9 spacecraft arrived at Mars, Sagan proposed that Mars might undergo massive climatic change over substantial periods of geological time, and that there may have been instances when martian climatology permitted abundant surface liquid water. Both discussions (Lederberg and Sagan, 1962; Sagan, 1971) were primarily devoted to the question of life

on Mars and the possibility of microenvironments favorable for biology there, either in space or in time.

The Mariner 9 discovery, amply confirmed by Viking Orbiter data, of sinuous valleys on Mars put these earlier speculations on a firmer observational footing (McCauley et al., 1972; Milton, 1973; Sagan, Toon and Gierasch, 1973; Baker and Milton, 1974; Sharp and Malin, 1975; Pieri, 1976; Malin, 1976; Masursky et al., 1977). Arguments from terrestrial geomorphological analogy are consistent with the channels being produced by running water. These features include teardrop-shaped interior islands; braided channels; tributary branching ratios (Pieri, 1979); and shoreline morphology (Carr et al., 1976). However, many geomorphologically distinct units have been subsumed under the single descriptive word, "channels" (see, for example, Shapr and Malin, 1975), and it seems likely that there are several distinct categories of valleys on Mars, each with a quite separate mode of origin (Pieri, 1976). Alternative physical processes which have been proposed or at least mentioned in martian channel morphogenesis include liquid carbon dioxide (Sagan et al., 1973), surface structural cracks (Schumm, 1974), erosion by windblown sand (Sagan et al., 1973; Cutts et al., 1976) and liquid alkanes (Yung and Pinto, 1978). Each of these alternative ideas has serious problems, some of which have been described in the original papers proposing these ideas and some of which have been published elsewhere: and aqueous erosion has proved to be by far the most popular, although by no means a uniformly admired, explanation. Substantial debate has occurred in the literature and elsewhere on the extent to which presumptive

aqueous channels on Mars are the result of breakout flooding, rainfall production of dendritic branched networks, or liquid water modification of pre-existing morphology.

Sagan et al. (1973) plotted a histogram of the abundance of both large and small channels as a function of martian latitude and noted a striking concentration towards the equator and a very substantial decline in number density by middle latitudes. They argued that one implication of this result is that the martian channels are cut by a fluid whose melting point is achieved at characteristic martian equatorial temperatures, but that high latitudes on Mars are below the freezing point of this fluid. Of all cosmically abundant inorganic materials only water satisfies these conditions, and this argument therefore supports the aqueous hypothesis of martian channel morphogenesis. However, the observations of craters and other martian landforms as a function of latitude has uncovered the existence of a high latitude mantling (Soderblom et al., 1974). The mantling transition seems to occur rather more sharply than the histogram of channel distribution with latitude implies, but at least a significant part of the channel distribution function with latitude might be due to the high latitude obscuration of channels by the presumably aeolian mantling material. In addition both Mariner 9 and Viking Orbiter coverage are poorer at high latitudes, because of orbital constraints and the 1971-72 dust storm, raising the possibility of a strong observational selection in the histogram data. Moreover, since many of the channels are now known to be of the order of 1×10^9 years old (Soderblom et al., 1974; Pieri, 1976; Neukum and Wise, 1976) it is not the present temperature distribution

with latitude but that of a billion years ago which applies in consideration of the nature of any channeling fluid.

The present mean surface pressure of Mars is near the triple point pressure of water. The highest surface pressures of Mars in the deepest depressions are probably in the 10 mb range. At these pressures, open pools of pure liquid water rapidly evaporate or boil away, and the aqueous origin of martian channels has thereby been relegated to some past epoch when the global atmospheric pressure was significantly greater, the surface temperatures perhaps higher as well, and abundant surface liquid water hypothesized (Sagan et al., 1973 and many later papers). Proposed mechanisms for such climatic change include variations in the obliquity of Mars (Sagan et al, 1973; Ward, 1973; Burns et al., 1978); variations in solar luminosity (Sagan et al.,1973; Hartmann 1974); variations in the polar albedo (Sagan et al., 1973); and a past more massive reducing atmosphere with a substantial greenhouse effect (Sagan and Mullen, 1972; Sagan, 1977; Pollack, 1979). Each of these processes must, at the very least, be designed to provide a significant increment in the martian atmospheric pressure, generally speaking at least to some tens of mb. Estimates of the equivalent partial pressure of volatiles frozen in the martian polar caps range from about one bar (Sagan, 1971) to close to zero (Ingersoll, 1974). Much larger quantities of volatiles seem to be trapped as subsurface permafrost, as chemically and physically bound water and as carbonates (Pollack et al., 1971; Fanale and Cannon, 1971; Houck et al., 1973; Biemann et al., 1976). $^{14}N/^{15}N$ and noble gas abundance ratios in the present martian atmosphere, as determined from the Viking entry mass spectrometer and surface gas chromatograph/mass spectrometer experiments, combined with models of

exospheric escape, suggest an earlier atmosphere with total pressure of tens of mb and possibly larger (McElroy et al., 1976; Anders and Owen, 1978). These results make it at least moderately plausible that martian global atmospheric pressure in its distant past, and perhaps even at 1×10^9 years ago, may have been high enough to reasonably stabilize aqueous fluvial processes in the open air -- enough to produce at least some of the martian sinuous channels.

Evaporation on Mars

However, what seems not to have been thoroughly investigated is the possibility that evaporation from an aqueous flow on Mars under present or even lower atmospheric pressure produces a surface layer of ice which inhibits subsequent evaporation and permits the subsurface flowing water to travel substantial distances and be responsible for major fluvial erosion. If martian rivers can flow under contemporary conditions in this way, flow under high pressures would be even more substantially enabled. The origin of major sinuous channels in chaotic terrain powerfully connects the idea of subsurface liquid water on Mars with the production of martian channels, even if such channels are generally massive outbreak flooding such as the Bonneville Event (Baker and Milton, 1974) -- that is, largely a surface, not a subsurface, flow.

Ingersoll (1970) has shown that the present low atmospheric pressure on Mars greatly enhances evaporation, so that snow and frost deposits sublime instead of melting. rainfall cannot occur. Ingersoll's

objection to the presence of liquid water on Mars does not apply if the water is provided by some other means, such as geothermal heating of buried ice deposits, where the overlying soil prevents evaporation. If such water were to be exposed to the martian atmosphere, as groundwater issuing from a spring, it would begin to evaporate rapidly, and boil if its vapor pressure exceeded the local atmospheric pressure, and possibly effervesce as well if it contained dissolved gases. The rapid cooling due to the release of the latent heat of evaporation will cause a layer of ice to form and grow in thickness. The result would resemble a terrestrial stream in winter, except that the cooling of the martian stream would be mainly by evaporation. Lingenfelter et al. (1968; see also Schubert, et al., 1970) have studied a similar scenario on the Moon, in which water is exposed to the lunar vacuum. They argued that the lunar rills might have been produced by water erosion in a manner similar to the origin of terrestrial river valleys. The remarkably anhydrous character of the lunar regolith and the absence in lunar rills of many of the characteristic morphological forms of aqueous erosion on Earth (or Mars) has led to the general opinion that lunar rills are generated in some other way, perhaps as collapsed lava tubes. However, the calculations of Lingenfelter et al., which require a head of lunar liquid water, are not invalidated by this evidence, and can be applied to the much more hydrated martian conditions if evaporation rates and solar heating appropriate to the martian environment are substituted.

Because of the large latent heat of evaporation of water and ice, any calculation of evaporation rates must take into account the strong interaction of the evaporative cooling by escape of vapor, the temperature of the surface of the ice

which controls the vapor pressure, and the supply of heat to the surface layer by insulation from above and thermal conduction from the water below. The evaporation and energy balance equations used by Lingenfelter et al., are given below in a slightly modified form.

For the upper and lower boundaries, respectively, of the ice layer,

$$E_u = (1 - f)q_i + q_c - \sigma T_u^4 - L_s\dot{m}_u \qquad (1)$$

$$E_\ell = fq_i - q_c + L_f\dot{m}_\ell \qquad (2)$$

where E_u = the energy flux to the upper ice surface; E_ℓ = the energy flux to the lower ice surface; $\dot{m}_u$ = the evaporation rate from the upper surface; $\dot{m}_\ell$ = the rate of freezing at the lower surface; σ = the Stefan-Boltzmann constant; T_u = the temperature at the upper surface; q_c = the conductive heat flux through the ice; q_i = the flux of sunlight that is absorbed within the ice layer; and f = the fraction of q_i that is absorbed beneath the ice layer. The situation is presented schematically in Figure 1. As the ice sheet grows in thickness, it approaches an equilibrium at which

$$E_u = E_\ell = 0 \qquad (3)$$

$$\dot{m}_u = \dot{m}_\ell \; ; \qquad (4)$$

in other words, at which the ice sheet is constant in thickness and is characterized by a constant net energy flux.

The parameter f is introduced to take into account the transparency of the ice layer. If the ice were completely transparent (f = 1), all the solar energy which penetrates the ice would be absorbed in the water below and must be carried back up to the surface by conduction through the ice, resulting in the minimum possible ice thickness. On the other hand, if the ice layer were dirty and opaque throughout, or covered with a thin layer of soil, f would be 0, and the maximum possible ice thickness at equilibrium would be reached. All cases with partial transmission of the incident sunlight or absorption throughout the ice layer will produce equilibrium ice thicknesses between these two extremes.

Calculation of the conductive heat flux q_c cannot be done in the simple fashion of Lingenfelter et al. because the heat conductivity of ice varies with temperature. According to the data of Ratcliffe (1962), the thermal conductivity of ice can be well represented between 120°K and the melting point by the equation:

$$k(T) = (1.863/T) - 0.00147 \text{ cal cm}^{-1}\text{s}^{-1}(\text{K}^{\circ})^{-1}, \qquad (5)$$

where T is the absolute temperature. The one-dimensional steady-state thermal conduction equation

$$q_c = k(T)\ (dT/dx) \qquad (6)$$

can now be integrated to yield

$$q_c = [1.863\ \ell n\ (273.15/T_u) - 0.00147(273.15-T_u)]/\Lambda \qquad (7)$$

where Λ is the thickness of the ice layer.

The calculation of the evaporation rate of water and ice under martian conditions is complicated by the fact that three different physical regimes are involved, depending on the atmospheric pressure and the wind speed. The most straightforward regime is evaporation into vacuum, which was used as the boundary condition by Lingenfelter et al. in their study of evaporation on the moon. The evaporation rate (g $cm^{-2}s^{-1}$) into a vacuum can be derived from simple considerations of kinetic theory, except for a numerical coefficient, and is given by Kennard (1938) as

$$\dot{m} = \alpha(p_v - p_a)(M/2\pi RT)^{\frac{1}{2}} \qquad (8)$$

where p_v = the vapor pressure of the ice or water; p_a = the atmospheric pressure; M = the molecular weight of the vapor; R = the universal gas constant; and α = the coefficient of evaporation. The value of α must be determined empirically. Tschudin (1946) has found a value of 0.94 ± 0.06, or essentially unity. This equation for the evaporation rate is valid only if $p_v > p_a$. When $p_v < p_a$, the escape of the vapor from the surface is governed by diffusion rather than by effusion, and other considerations apply.

Since atmospheres are seldom if ever completely still, the next physical regime to consider is evaporation by wind. A number of theories of evaporation by wind which have been proposed were tested by Marciano and Harbeck (1954) using data taken in a study of evaporation from a reservoir. They found that their data were best represented by a formula derived by Sverdrup (1937). Sverdrup assumes that the effect of the wind is to divide the atmosphere into two layers in which two different transport processes are dominant. Next to the surface is a laminar boundary layer in which water

vapor transport is by molecular diffusion. Above this layer the air flow becomes turbulent, and eddy diffusion is the dominant means of vapor transport. The thickness, d, of the laminar sublayer is roughly

$$d = 30\nu/u_* \tag{9}$$

where u_* = the friction velocity of the wind; and ν = the kinematic viscosity of the atmosphere. Above the laminar sublayer, the eddy diffusivity is found to be given by

$$K(z) = \kappa u_* (z + z_0), \tag{10}$$

where K(z) = the eddy diffusivity at height z; κ = the von Karman constant $\simeq 0.40$ empirically; z = the height above the surface; and z_0 = the roughness length characteristic of the surface. The evaporation formula can now be obtained by integrating the inverse of the diffusivity between the surface and some height Z, to give

$$\dot{m} = \frac{\Delta\rho}{\int_0^d \frac{dz}{D} + \int_d^Z \frac{dz}{K(z)}} = \frac{\Delta\rho}{\frac{d}{D} + \frac{1}{\kappa u_*} \ln\left[\frac{Z+z_0}{d+z_0}\right]} \tag{11}$$

where D = the diffusion coefficient of water vapor; and $\Delta\rho$ = the difference in the water vapor density between the surface and height Z.

Before any calculations of actual evaporation can be made, it is necessary to evaluate the physical constants which appear in the previous equations, and to discuss their physical significance. The value of the diffusion coefficient D of water vapor in a pure carbon dioxide atmosphere is obtained from the data of Schwertz and Brow (1951), taken at atmospheric

pressures. Assuming that the diffusion coefficient varies as $T^{3/2}$ and p^{-1}, the value

$$D = 0.1654\ (T/273.15)^{3/2}\ (1013\ mb/p)\ cm^2 s^{-1} \qquad (12)$$

is obtained, where p is here measured in millibars. The dynamical viscosity η of carbon dioxide is taken from the experimental results of Sutherland and Maass (1932), and of Johnston and McCloskey (1940). A least squares polynomial fit to their data yields

$$\eta = (0.002162\ T^2 + 3.771\ T + 172.01)\ x\ 10^{-7}\ dyne\ s\ cm^{-1} \qquad (13)$$

and the kinematic viscosity ν is obtained by dividing by the density of the gas.

The value of the roughness length z_0 is determined by aerodynamic measurements, and is typically found to be about 1/30 of the physical scale of the roughness elements on the surface. Thus a region such as the Chryse landing site of Viking 1 (Mutch et al., 1976) which has boulders and sand drifts about 1 meter in size would thereby have a roughness length of about 3 cm. Such roughness in a martian river would resemble a terrestrial ice jam, and would not be likely to occur unless the current were very strong, or some other phenomenon such as a seasonal thaw occurred to break up an existing ice sheet. On the other hand, if the roughness length of the Chryse landing site were determined by the abundant rocks in the decimeter to centimeter scale the roughness length would be millimeter to submillimeter. Except for massive outbreak floods, one would expect the ice surface to resemble more

the ice on a terrestrial stream in winter, smooth enough, if not thick enough, to skate on, since the physics of ice break-up would be the same on Mars and not dependent on any novel evaporation physics.

It is somewhat a matter of guesswork to pick an appropriate value for the roughness length of a smooth ice sheet, but this will be shown later not to be of critical importance. For comparison with terrestrial values, Sverdrup (1937) finds $z_0 = 0.6$ cm for the ocean, and Marciano and Harbeck (1954) find similar values for the reservoir used in their studies. For solid surfaces the roughness length is considerably smaller, 0.1 cm for a snow surface on a prairie, 0.005 cm for smooth snow on short grass, and 0.001 cm for smooth mud flats (Priestley, 1959). For the purpose of this calculation, it will be assumed that $z_0 = 0.1$ cm for the surface of the ice sheet on a martian river, since larger values seem unlikely and smaller values will be shown to be unimportant to the calculations.

The wind profile, which relates the friction velocity u_* and the physical wind velocity u as a function of height is either dominated by the surface roughness or by the atmospheric viscosity, depending on whether the friction velocity is greater or less than the critical velocity (Priestley, 1959, pp 19-20):

$$u_{*c} = 2.5\ \nu/z_0 \qquad . \qquad (14)$$

In the former case, the flow is aerodynamically rough, and the turbulent eddies are able to reach the surface , so the wind profile is given by

$$u/u_* = (1/\kappa)\, \ell n(z/z_0) \quad . \qquad (15)$$

In the latter case the flow is aerodynamically smooth, and viscous dissipation prevents the eddies from reaching the surface; the wind profile is then given by

$$(u/u_*) = 5.5 + (1/\kappa)\, \ell n(u_* z/\nu) \quad . \qquad (16)$$

For typical martian conditions ($p = 6$ mb, $T = 200^{\circ}K$, $\nu = 6.4$ cm^{2}s^{-1}), the air flow will be rough over regions like the Viking 1 landing site ($z_0 = 3.3$ cm) for $u_* \geq 5$ cm s^{-1}. According to Hess et al. (1976) the Viking 1 anemometer at a height of 160 cm always registered wind speeds greater than about 100 cm s^{-1}, which indicates that the air flow is always aerodynamically rough, since $u(160 \text{ cm})/u_* = 9.7$ from the approximate wind profile (15). In contrast, the air flow over the ice sheet would almost always be smooth; the critical friction velocity from equation (14) must exceed 160 cm s^{-1} for the flow to become rough. This is very near the wind velocity calculated by Sagan and Bagnold (1975) at which large quantities of dust become airborne to produce sandstorms. Since such storms occur only a few days per year, the airflow over the ice surface can be considered almost always to be smooth. Any smaller value for the roughness length of the ice sheet would only increase the critical friction velocity of the wind, and strengthen the assumption of laminar flow. Thus we have confidence in the applicability of the analysis of Sverdrup (1937), which assumes the existence of a laminar sublayer.

The values of $\Delta\rho$ and Z in equation (11) present minor difficulties in applying the evaporation formula to Mars, since the water vapor density must also be measured at some height Z. If the air blowing over the ice sheet is assumed to be completely dry, $\Delta\rho$ is obviously the saturation vapor density at the surface of the ice. The height Z at which the atmosphere is assumed to be completely d is not as obvious, but may be estimated by considering the horizontal as well as the vertical transport of the water vapor by the wind. By equating the time scale for the vapor to diffuse to a height Z with the time scale for the wind to blow across the horizontal extent of the ice sheet X, the relation

$$T = Z/v = X/u(Z) \tag{17}$$

is obtained, where V is some characteristic velocity of the diffusion process. On dimensional grounds,

$$V = \frac{\dot{m}}{\Delta\rho} = \frac{1}{\frac{d}{D} + \frac{1}{\kappa u_*} \ln\left[\frac{(Z+z_0)}{d+z_0}\right]} \tag{18}$$

Employing the wind profile of equation (16), we obtain a relation between Z and X:

$$X = \frac{Zu(z)}{V} = Zu_* \left[5.5 + \frac{1}{\kappa} \ln\left(\frac{u_* z}{\nu}\right)\right]\left[\frac{d}{D} + \frac{1}{\kappa u_*} \ln\left\{\frac{Z+z_0}{d+z_0}\right\}\right] \tag{19}$$

Even small assumed values of Z result in large values for X, as is shown in Table 1.

	Z = 50 cm	Z = 100 cm
$u_* = 10$ cm s^{-1}	X = 109 m	X = 235 m
$u_* = 30$ cm s^{-1}	X = 154 m	X = 326 m
$u_* = 100$ cm s^{-1}	X = 210 m	X = 442 m

Table 1.

The choice of Z obviously depends on the width X of the river or lake that is evaporating, and some of the martian channels are observed to be hundreds of meters to kilometers in width. The evaporation rate, however, depends only weakly on Z, since it appears only logarithmically in equation (11). In subsequent calculations, Z will be taken to be 1 meter, since this is of the right order of magnitude, and the evaporation rate is insensitive to small differences in Z.

The third physical regime we consider is evaporation in the absence of wind. Ingersoll (1970) has shown that evaporation can also take place in the absence of wind by free convection, since the atmosphere near the ground which is saturated with water vapor is less dense than the overlying dry CO_2 atmosphere and is therefore dynamically unstable. Using the analogy between this situation and thermal convection above a heated horizontal surface, Ingersoll obtains for the evaporation rate

$$\dot{m} = 0.17\ \Delta\rho\ D \left[\frac{(\Delta\rho/\rho)\ g}{\nu^2}\right]^{1/3} \qquad (20)$$

where g is the gravitational acceleration and $\Delta\rho/\rho$ is the ratio of the

density difference produced by the water vapor in the atmosphere to the atmospheric density itself, given by

$$\Delta\rho/\rho = \frac{\left(m_c - m_w\right) p_v}{m_c p_a - \left(m_c - m_w\right) p_v} \quad , \tag{21}$$

where m_c = the molecular weight of CO_2 = 44; and m_w = the molecular weight of water vapor = 18. Equation (20) is valid only in the case of neutral thermal stratification, and the driving term, $\Delta\rho/\rho$, must be modified if the stratification is not neutral, since the temperature also affects the gas density. This effect is important but cannot easily be taken into account without a detailed study of the martian atmospheric temperature profile throughout the day, as was done by Gierasch and Goody (1968). They show that the martian atmosphere alternates between highly stable and highly unstable stratification daily, so that equation (20) can, at most, be used on a daily average basis. Measurements of the temperature difference between the ground and the air by Viking 1 (Hess et al., 1976) provide a rough measurement of the stratification effects near the ground. Near local noon, a maximum temperature difference of 25°K develops between the air and ground temperatures, giving $\Delta T/T = 0.1$. Substituting this for the driving term $\Delta\rho/\rho$ in equation (20) we derive an evaporation rate due to thermal convection corresponding to that produced by a wind with $u_* = 50$ cm s^{-1}. Winds of this velocity do blow near noon, and the evaporation of water from moist martian soil would certainly be enhanced by the addition of thermal convection to the turbulence produced by the wind. The evaporation rate of an ice sheet, however, would not be nearly as strongly affected by thermal convection, for several reasons. First, the greater thermal inertia of ice as compared to soil would reduce the diurnal

temperature variation of the top layer of the ice sheet. Second, the incident solar radiation which penetrates the ice layer would melt the bottom few centimeters of the ice during the day, which would then refreeze at night. If the ice sheet were more than about 10 cm thick, there would be only a negligible effect on the surface temperature of the ice. Third, the ice layer would probably have a higher albedo than the martian soil, further reducing the solar heating which leads to thermal convection. In their studies of terrestrial evaporation, Marciano and Harbeck (1954) found little if any effect of atmospheric stability on evaporation, probably for reasons similar to the first and second reason we have just given. In subsequent calculations, the effect of diurnal variations on thermal stability of the martian atmosphere will be neglected since they are probably small; they are in any case beyond the scope of this investigation.

Marciano and Harbeck (1954) report that small amounts of evaporation do take place in the absence of wind, and it seems reasonable to attribute this to free convection as proposed by Ingersoll (1970), rather than thermal convection -- since the stability of the atmosphere on Earth does not have a noticable effect on the evaporation rate. Since wind and free convection both seem to influence evaporation perceptably, the simplest approach to include them both would be to add their effects. Our proposed evaporation equation is thus the sum of equations (11) and (20), giving

$$\dot{m} = \frac{\Delta\rho}{\frac{d}{D} + \frac{1}{\kappa u_*} \ln\left(\frac{Z+z_0}{d+z_0}\right)} + 0.17\ \Delta\rho\ D \left[(\Delta\rho/\rho) g\ \nu^{-2}\right]^{1/3} \qquad (22)$$

where $\Delta\rho/\rho$ is given by equation (21). Equation (22) obviously has the correct behavior in the two limiting cases of high wind and negligible convection, and of convection in the near absence of wind, and makes the reasonable prediction that, when both wind and free convection are present, the result evaporation will be greater than that due to either cause alone. Accordingly, equation (22) will be used in the subsequent calculations in this investigation, with attention paid to whether one evaporation mechanism is clearly dominant, or a mixed case prevails. Equation (22) should apply as well to evaporation in many other planetary or satellite atmospheres, including those in the outer solar system.

Calculations were carried out for a variety of wind speeds, from dead calm to winds typical of sandstorm conditions ($u_* = 300$ cm s^{-1}) at a variety of pressures. A summary of the energy balance used in these calculations is shown in Figure 1. Evaporation rate as a function of insolation is displayed in Figure 2 for the mean martian pressure of 6 mb as well as for a vacuum, and for a range of values of u_*. For typical martian insolations the ice evaporation rate is typically between 10^{-6} and 10^{-8} gm $cm^{-2}s^{-1}$. At 6 mb pressure, a reasonable range in martian wind velocities corresponds to about 1.5 orders of magnitude in the evaporation rate. The effect of other choices of atmospheric pressure on the evaporation rate for the case $u_* = 0$ is shown in Figure 3. These graphs can be used to make a rough interpolation for other values of p and u_*. If 3 mb corresponds to typical elevations on Mars and 9 mb to typical depressions, we see that the pressure variation amounts to more than a factor of three in the evaporation rate for

typical insolations. On the other hand, evaporation rates are retarded over the vacuum rate by more than two orders of magnitude for 6 mb pressure, by more than three orders of magnitude for 100 mb, and by almost 4 orders or magnitude for one bar pressure. Corresponding values of the dependence of the minimum thickness of ice ($f=1$) under these circumstances, for a range of values of insolation and total pressure, on u_* are shown in Figures 4 and 5. In all cases of interest the thickness of the ice overburden exceeds one meter. We see that the minimum ice thickness at typical values of martian atmospheric pressure is a few times less than that which would be required at equilibrium under vacuum conditions. In Fig. 6 is the maximum ice thickness obtained by setting $f=0$ in eqs. (1) and (2), assuming the equilibrium conditions (3) and (4) and employing eq. (22). Typical values range from 10 to several hundred meters, compared to about 1 m. for the minimum case. For plausible values of f, p, u and insolation, the ice thickness seems to be $\sim$10 to 30 m, less than but a significant fraction of the depths of large Martian channels. Ice-covered rivers swept free of overlying dust, perhaps channelled winds, will have minimum ice covers; such rivers with a thick coating of dust or sand will approach maximum ice covers. Thus the most dramatic cases tend to be the most difficult to detect.

Lifetime and Present Detectability of Ice-Covered Rivers

If geothermal melting of subsurface ice and permafrost is the mechanism for producing at least a subset of martian sinuous channels, such channels should have been preferentially generated in times of high geothermal activity. The peak epoch of martian volcanism and tectonic activity dates to about 1×10^9 years ago, the era of the formation of the volcanic structures in Tharsis and the adjacent Vallis Marineris. Since this is also the epoch of the formation of most of the martian channels, the ice-covered river hypothesis is at least consistent with the available chronologies. With the density of water as a normalization factor, the minimum lifetime of a martian ice-covered river is of the order of $\delta/\dot{m}$, where δ is the depth of the river. Thus, for $\delta \sim 10^4$ cm and $\dot{m}$ $\sim 10^{-8}$ gm cm^{-2}s^{-1}, $t \gtrsim 10^{12}$ s $\sim 3 \times 10^4$ yrs. Such a value of t applied strictly only to a terminal lake and should be a very low lower limit to the river lifetime, which

will depend crucially on the time dependence of the discharge Q. By comparison, the lifespan of the Colorado River in the Grand Canyon is $\sim 10^7$ years. A rough estimate suggests that there are on Mars several x 10^5 sinuous channels, including those covered by aeolian and other mantling. In the highly idealized circumstance that the construction of such channels was distributed uniformly over martian history from the major events of 1 x 10^9 years ago to today, there would be on the average >>10 ice-covered rivers present at any given time. Since initiating geothermal events were probably concentrated back around 1 x 10^9 years ago the actual number in the present epoch should be less; but such calculations suggest that there might be several such rivers on Mars at the present time. In Fig. 7 is calculated the equilibrium temperature at the top of the ice sheet, given by eqs. (1) through (4) and independent of the evaporation eq. (22). The vacuum case [eq. (8)] is also shown. Thus, a contemporary ice-covered channel would be characterized by a high albedo and a temperature around 210 to 235° K, with only modest diurnal and seasonal temperature excursions. Because of the dependence of $\dot{m}$ on the insolation, such channels might be preferentially present at high latitudes.

Subsurface Lakes and Polar Laminae

In the previous calculations it was found that liquid water exposed to martian conditions will shield itself against evaporation by forming a layer of ice 1 m or more thick. What will happen to an initially solid layer of ice, such as the martian polar caps, due to the heating from sunlight? Will enough sunlight penetrate deep into the ice to cause subsurface melting, or will the ice sheet remain frozen throughout? The answer to this question depends critically on the amount of insolation, and the transparency of the ice. If the sunlight penetrating the ice is assumed to be absorbed exponentially with a characteristic length L, the steady-state one-dimensional heat conduction equation becomes

$$q_c(x) = k(T)(dT/dx) = q_i \exp(-x/L), \qquad (23)$$

where q_c is the conductive heat flux at depth x, and q_i is the incident solar energy flux that is absorbed. Using the expression for k(T) in equation (5) the equation can be integrated to give

$$1.863 \ln(273.15/T_s) - 0.00147(273.15-T_s) = q_i L \left[1-\exp(-x/L)\right] \qquad (24)$$

where T_s is the surface temperature of the ice. Melting can only occur at depths greater than the value of x which satisfies the equation. If x is allowed to go to infinity, a critical value of L can be found below which exogenous melting is not possible because the sunlight cannot penetrate deeply enough into the ice. Assuming a surface temperature of the ice of 180°K (the average of the summer temperature of 210°K and the winter temperature of 150°K), a polar cap albedo of 0.5, and the insolation of the poles at the summer solstice, with a solar elevation of 24°, the critical value of L is 220 cm. For the yearly average insolation, the maximum insolation must be reduced by a factor of π, and L becomes 700 cm. These numbers represent reasonable transparencies, provided the ice is not dirty or opaque because of air bubbles. Thus, it seems plausible to expect that subsurface melting may occur in the martian polar caps, either on a seasonal or a permanent basis.

One objection which might be made to our proposed subsurface melting is that it does not occur at least often on Earth in the Greenland and Antarctic ice caps. More sunlight reaches the Earth than Mars, and the yearly average surface temperature of the ice is here more like 240°K than 180°K, producing less conductive heat loss to the surface. There are several reasons that

this objection may be invalid. First, the polar regions on Earth are frequently cloudy, reducing the available insolation. Second, the albedo of snow is considerably higher, 0.8 or more, than the typical albedo of the martian polar caps, ≈ 0.5 or less. Third, Rayleigh scattering in the Earth's atmosphere further attenuates sunlight in the polar regions, especially at large solar zenith angles. Fourth, ice in the martian polar caps may be more transparent than in terrestrial glaciers because air bubbles may be smaller there or absent. The lower air pressure on Mars causes less air to be trapped in the void space between snowflakes (if it does snow on Mars), and this air is very easily compressed by the weight of overlying snow or ice. For pressure to reduce the volume of trapped air by one half, an ice layer 10 meters thick is needed on Earth. For Mars, this thickness is 20 cm. If snow does not fall on Mars, and ice is deposited as hoarfrost, less void space would be expected than for snow. Furthermore, the air bubbles may disappear completely because of the formation of clathrate ice. Such a disappearance happens on Earth only deep in glaciers, but can happen at much lower pressures on Mars because of the comparative ease of formation of CO_2 clathrate. The transmission of light through ice on Mars would be less dominated by scattering from air bubbles than on Earth, and more by the natural light absorption of the ice, and by absorption produced by any dust particles trapped in the ice.

Permanent ice-covered bodies of liquid water are known to exist in Antarctica (Lipps et al., 1977; Anonymous, 1977), but are almost certainly not heated by insolation. Two hundred meters thickness of liquid water have been found in a subsurface lake in the Ross Ice Shelf beneath 420 m of ice. The coldest water was found to be about 100 m from the lake bottom, suggesting that some melting is occurring at

the bottom of the ice layer. There is some evidence that this water/ice equilibrium has been maintained for more than 10^5 years.

It is conceivable that these ideas have some bearing on the origin of the martian polar laminae (Murray et al., 1972; Cutts, 1973; Soderblom et al., 1973; Cutts et al., 1976; Howard, 1978), where the individual plates or laminae are between meters and tens of meters thick (Dzurisin and Blasius, 1975). Ward (1973) has shown that the obliquity of Mars varies between about 15° and 35°, the current value being 24°, over time scales of a hundred thousand years or more. In a past epoch of higher obliquity, extensive subsurface melting could have produced a large polar lake on which a layer of ice floated. Any irregularities in surface topography would be reduced by the iceberg effect, and then eliminated by melting of the bottom of the icebergs. In a subsequent epoch of low obliquity, the polar lake would freeze, producing a level surface like that observed in each of the polar laminae. We propose that repetitions of this cycle, with surface deposition of ice between intervals of melting, could have produced the observed stacked laminae. While the smoothness of the laminae may have many conceivable explanations, including aeolian ones, the most natural mechanism for producing a smooth surface is liquification.

The largest impact crater on either martian cap is designated Zw, in the Planum Boreum at 85° North latitude, 180° West. It is adjacent to the Chasma Boreale, a very large valley, one to two kilometers below the surrounding elevations and directed at Zw. We speculate that the proximity of these two features has a genetic origin, with the crater impact that produced Zw releasing a large body of subsurface water which produced the Chasma Boreale.

The lower limit to the observed thickness of individual laminae is about 5 m (Dzurisin and Blasius, 1975), although finer scale laminae may exist, below the effective slant resolution of the Mariner 9 high resolution camera for martian polar latitudes. We note that the thickness of our ice overburden on such subsurface lakes is of just the same order as the inferred lamina thickness.

Flow Discharge in Martian Channels

An ice-covered river of total area A and surface evaporation rate $\dot{m}$ will lose a total mass of water to the atmosphere of $A\dot{m}$ grams every second.

This mass of ice lost from the top surface is reformed by freezing at the bottom surface so the net loss is to the liquid water. Because water has a density of 1 g cm^{-3}, the steady state situation is maintained if the river is characterized by a discharge $Q = A\dot{m}$. If the discharge is larger than $A\dot{m}$, then the arrival flux of liquid water through a vertical surface beneath the ice is greater than what is lost by evaporation and the head waters of the river make progress in channel erosion. The values of $\dot{m}$ derived above are extremely low. For $\dot{m} \sim 10^{-6}$ gm $cm^{-2}s^{-1}$ and $A \sim 10^{11}$ cm^2 the discharge for evaporative equilibrium must be only of the order of 10^5 cm^3s^{-1}. For comparison the mean annual Q in typical terrestrial river systems is $\sim 10^7$ to 10^{10} cm^3s^{-1} and estimated peak discharges for the Missoula and Bonneville floods is $\sim 10^{13}$ cm^3s^{-1} (Malde, 1968; Baker, 1973). Very crude estimates for Ares Vallis on Mars during its formation give a peak discharge $\sim 10^{14}$ cm^3s^{-1} (Masursky et al., 1977).

Thus, it is clear that large values of Q will propagate extensive flood and channel systems on Mars even for very low values of p and for very high values of u_*. There is no problem in understanding massive breakout floods on Mars under any conceivable past or present climatic conditions. In addition, if geothermal penetration of subsurface ice or permafrost has, at least on a few occasions on Mars, produced catastrophic floods connected with the chaotic terrain, there must have been large numbers of other geothermal events which produced more modest erosion which seems very likely to have formed ice-covered rivers and ultimately sinuous channels. It is clear from the evaporation rates calculated in the present paper that even with modest discharges of $10^5 cm^3s^{-1}$ or even smaller such rivers could have had reaches

comparable to those of the existing sinuous channels on Mars. Even dendritic valley networks of the sort which Masursky et al. (1977) attribute to rainfall can have originated as ice-covered rivers if geothermal penetration occurred in several adjacent locales which eventually became the headwaters of the distributaries. It is not clear that under these circumstances distinctive morphological features would be present at these locales today. Our arguments by no means exclude the possibility of the production of sinuous channels by rainfall in earlier more clement times, but we note that the higher atmospheric pressures and lower wind velocities expected for such times make the efficiency of the processes we have described here more efficient in those clement environments. Masursky et al. (1977) have argued that our ice-covered river mechanism could not explain the broad martian channels because, they claim, the discharges necessary to produce such river beds are very high, which would imply turbulent flow and a lack of contact between the water and its ice overburden -- thereby fragmenting the ice cover. However, the frictional drag of the ice in a turbulent river would be small, and we have found the steady state ice thickness to be a significant fraction of the depth of the river; in addition, as shown immediately above, the discharge rates required in this problem may be very modest and laminar flow regimes might prevail, especially in highly evolved systems with low Q. Also, such ice-covered subsurface rivers are self-sealing. Some subsurface percolation at the headwaters of such streams should occur; but since the mean temperature of Mars is well below the freezing temperature of water at locales far from the initiating geothermal events, the ground will be frozen and percolation will be minimal. Heat transport from the headwaters heated by the hypothesized geothermal event to the colder ground at the lowest instantaneous elevation of the flow can be expected to aid stream bed erosion. Clark (1978), in discussing our model, proposes that the bottom surface of the underground stream may freeze because of conduction with the cold soil and that the resulted reduced

friction-to-flow would advance the reach of the system; he also proposes that the heat of wetting and the heat of solution at least by anhydrous minerals might contribute to the heat transport.

Exobiological Implications

The objective of the original speculations about subsurface lakes (Lederberg and Sagan, 1962) and surface bodies of water (Sagan, 1971) was their suitability as abodes of indigenous life for aqueous biochemistries similar to those on Earth. The Viking 1 and 2 Landers performed preliminary searches for life in two martian locales totally devoid of liquid water. No hint of martian macrobes was uncovered (Mutch et al., 1976; Levinthal et al., 1977); the search for martian microbes in the same locale has given results which are tantalizing but at best ambiguous (Klein, 1978). The Viking experiments tested for life in one corner of the water activity/temperature diagram of Sagan and Lederberg (1976), who also suggested that there may be a selective advantage for large organisms on Mars -- including ones with aqueous biochemistries. We now recognize that extensive regions of subsurface liquid water may exist on contemporary Mars, as in the past. Chaotic terrain and the most recent polar laminae are two candidate locales for future biological investigation of Mars. We note that the sequestered sub-ice sea, isolated from its aqueous surroundings probably for $>10^5$ years, recently investigated by the Ross Ice Shelf Project (Anonymous, 1977) turns out to have a rich population of arthropods, foraminifera and bacteria with some evidence for diatoms and marine worms, in an environment whose abyssal reaches, at least, exclude photosynthesis. The history of the exploration of Mars suggests that preliminary observations of limited surface areas may lead incautious investigators to concludsions which are not

applicable to all regions of the planet. The search for contemporary ice-covered rivers, probably of short reach, and subsurface lakes -- perhaps associated with high thermal inertias -- would be a useful first step in exploring the liquid water heterogeneity of Mars. The search for subsurface aqueous regimes beneath an overburden of one or a few meters of ice seems an ideal objective for the use of high velocity penetrators launched from orbiting spacecraft. Investigations of recent sinuous channels or chaotic terrain seem to be excellent objectives for roving vehicles and low altitude martian aircraft modeled after existing competition gliders.

Acknowledgments

This research was supported by the Planetary Geology Program, NASA Headquarters under Grant 33-010-220. We thank Peter Gierasch and David Pieri for stimulating conversations and Bonnie Buratti for assistance.

REFERENCES

Anonymous (1977). Life beneath the Antarctic Sea. Science News 112, 421.

Anders, E., Owen, T. (1978). Mars and earth: Origin and abundance of volatiles. Science 198, 453-465.

Baker, V.R. (1973). Paleohydrology and sedimentology of Lake Missoula flooding in Eastern Washington. Geol. Soc. Amer. Spec. Pop. 144, 79.

Baker, V.R., Milton, D.J. (1974). Erosion by catastrophic floods on Mars and earth. Icarus 23, 27-41.

Belcher, D., Veverka, J., and Sagan, C. (1971). Mariner photography of Mars and aerial photography of earth: Some analogies. Icarus 15, 241-252.

Biemann, K., Oro, J., Toulmin III, P., Orgel, L.E., Nier, A.O., Anderson, D.M., Simmonds, P.G., Flory, D., Diaz, A.V., Rushneck, D.R., and Biller, J.A. (1976). Search for organic and volatile inorganic compounds in two surface samples from the Chryse Planitia region of Mars. Science 194, 72-76.

Carr, M.H., Masursky, H., Baum, W.A., Blasius, K.R., Briggs, G.A., Cutts, J.A., Duxburry, T., Greeley, R., Guest, J.E., Smith, B.A., Soderblom, L.A., Veverka, J., and Wellman, J.B. (1976). Preliminary results from Viking orbiter imaging experiment. Science 193, 766-776.

Carr, M.H., Greeley, R., Blasius, K.R., Guest, J.E., and Murray, J.B.(1977) Some Martian volcanic features as viewed from the Viking orbiters. J. Geophys. Res. 82, 3985-4015.

Carr, M.H., Schaber, G.G. (1977). Martian permafrost features. J. Geophys. Res. 82, 4039-4054.

Clark, B.C. (1978). Implications of abundant hygroscopic minerals in the Martian regolith. Icarus 34, 645-665.

Cutts, J.A. (1973). Nature and origin of layered deposits of the Martian polar regions. J. Geophys. Res. 78, 4231-4249.

Cutts, J.A., Blasius, K.R., Briggs, G.A., Carr, M.H., Greeley, R., and Masursky, H. (1976). North polar region of Mars: Imaging results from Viking 2. Science 194, 1329-1337.

Cutts, J.A., Blasius, K., and Farrell, K.W. (1976). Mars: New data on Chryse basin land forms (abstract). Bull. Amer. Astron. Soc. 8, 480.

Dzurisin, D., and Blasius, K.R. (1975). Topography of the polar layered deposits of Mars. J. Geophys. Res. 80, 3286-3306.

Fanale, F.P., and Cannon, W.A. (1971). Adsorption on the Martian regolith. Nature 230, 502-504.

Gierasch, P. and Goody, R. (1968). A study of the thermal and dynamical structure of the Martian lower atmosphere. Planet. Space Sci. 16, 615-646.

Hartmann, W.K. (1974). Martian and terrestrial paleoclimatology: Relevance of solar variability. Icarus 22, 301-311.

Hess, S.L., Henry, R.M., Leovy, C.B., Ryan, J.A., Tillman, J.E., Chamberlain, T.E. Cole, H.L., Dutton, R.G., Greene, G.C., Simon, W.E., and Mitchell, J.L. (1976). Preliminary meteorological results on Mars from the Viking 1 lander. Science 193, 788-791.

Houck, J.R., Pollack, J.B., Sagan, C., Schaack, D., and Decker, Jr., J.A. (1973). High altitude infrared spectroscopic evidence for bound water on Mars. Icarus 18, 470-480.

Howard, A. (1978). Origin of the stepped topography of the Martian poles. Icarus 34, 581-599.

Ingersoll, A.P. (1970). Mars: Occurrence of liquid water. Science 168, 972-973.

Johnston, H.L., and McCloskey, K.E. (1940). Viscosities of several common gases between 90°K and room temperature. J. Phys. Chem. 44, 1038-1058.

Kennard, E.H. (1938). Kinetic Theory of Gases, 1st edition. McGraw-Hill Book Co., New York.

Klein, H.P. (1978). The Viking biological experiments on Mars. Icarus 34, 666-67

Lederberg, J., Sagan, C. (1962). Microenvironments for life on Mars. Proc. Nat. Acad. Sci. 48, 1473-1475.

Levinthal, E.C., Jones, K.L., Fox, P., Sagan, C. (1977). Lander imaging as a detector of life on Mars. J. Geophys. Res. 82, 4468-4478.

Lingenfelter, R.E., Peale, S.J., Schubert, G. (1968). Lunar Rivers. Science 161, 266-269.

Lipps, J.H., Krebs, W.N., and Temnikow, N.K. (1977). Microbiota under Antarctic ice shelves. Nature 265, 232-233.

Malde, H.E. (1968). The catastrophic late Pleistocene Bonneville flood in the Snake River plain, Idaho. U.S. Geol. Surv. Prof. Pap. 596, 52 pp.

Malin, M.C. (1976). Age of Martian channels. J. Geophys. Res. 81, 4825-4845.

Marciano, J.J., and Harbeck, G.E. (1954). Mass transfer studies: H_2O loss investigations. Lake Hefner Studies Technical Report 1, 46-70. U.S. Geol. Sur. Prof. Pap. No. 269.

Masursky, H., Boyce, J.M., Dial, A.L., Schober, G.G., and Strobell, M.E. (1977). Classification and time of formation of Martian channels based on Viking data. J. Geophys. Res. 82, 4016-4038.

McElroy, M.B., Yung, Y.L., and Nier, A.O. (1976). Isotopic composition of nitrogen: Implications for the past history of Mars' atmosphere. Science, 194, 70-72.

Milton, D.J. (1973). Water and processes of degradation in the Martian landscape. J. Geophys. Res. 78, 3027-4047.

Murray, B.C., Soderblom, L.A., Cutts, J.A., Sharp, R.P., Milton, D.J., and Leighton, R.B. (1972). Geological framework of the South polar region of Mars. Icarus 17, 328-345.

Mutch, T.A., Binder, A.B., Huck, F.O., Levinthal, E.C., Liebes, Jr., S., Morris, E.C., Patterson, W.R., Pollack, J.B., Sagan, C., and Taylor, G.R. (1976). The surface of Mars: The view from the Viking 1 Lander. Science 193, 791-801.

Meukum, G., and Wise, D.U. (1976). Mars: A standard crater curve and possible new time scale. Science 194, 1381-1387.

Owen, T., Biemann, K., Rushneck, D.R., Biller, J.E., Howarth, D.W., and Lafleur, A.C. (1977). The composition of the atmosphere at the surface of Mars. Journal of Geophys. Res. 82, 4635-4639.

Pieri, D. (1976). Martian channels: Distribution of small channels on the Martian surface. Icarus 27, 25-50.

Pieri, D. (1979). Thesis, Cornell University. In preparation.

Pollack, J.B., Pitman, D., Khare, B.N., and Sagan, C. (1970). Goethite on Mars: A laboratory study of physically and chemically bound H_2O in ferric oxides. J. Geophys. Res., 75, 7480-7490.

Pollack, J.B., (1979). Climatic change on the terrestrial planets, Icarus, in press.

Priestley, C.H.B. (1959). Turbulent transfer in the lower atmosphere. U. of Chicago Press, Chicago.

Ratcliffe, E.H. (1962). The thermal conductivity of ice. New data on the temperature coefficient. Phil. Mag. 1, 1197-1203.

Sagan, C. (1971). The long winter model of Martian biology: A speculation. Icarus 15, 511-514.

Sagan, C. (1977). Reducing greenhouses and the temperature history of Earth and Mars. Nature 269, 224-226.

Sagan, C., and Bagnold, R.A. (1975). Fluid transport on Earth and aeolian transport on Mars. Icarus 26, 209-218.

Sagan, C., and Lederberg, J. (1976). The prospects for life on Mars: A pre-Viking assessment. Icarus 28, 291-300.

Sagan, C., and Mullen, G. (1972). Earth and Mars: evolution of atmospheres and surface temperatures. Science 177, 52-56.

Sagan, C., Toon, O.B., and Gierasch, P.J. (1973). Climatic change on Mars. Science 181, 1048-1049.

Sagan, C., and Young, A.T. (1973). Solar neutrinos, Martian rivers, and Praesepe. Nature 243, 459-460.

Schubert, G., Lingenfelter, R.E., and Peale, S.J. (1970). The morphology, distribution, and origin of lunar sinuous rilles. Rev. Geophys. Space Phys. 8, 199-224.

Schumm, S.A. (1974). Structural origin of large Martian channels. Icarus 22, 371-384.

Schwertz, F.A., and Brow, J.E. (1951). Diffusivity of H_2O vapor in gases. J. Chem. Phys. 19, 640-646.

Sharp, R.P. (1973). Mars: Fretted and chaotic terrain. J. Geophys. Res. 78, 4073-4083.

Sharp, R.P., and Malin, M.C. (1975). Channels on Mars. Geol. Soc. Amer. Bull. 86, 593-609.

Sharp, R.P., Soderblom, L.A., Murray, B.C., and Cutts, J.A. (1971). The surface of Mars 2. Uncratered terrains. J. Geophys. Res. 76, 331-342.

Soderblom, L.A., Condit, C.D., West, R.A., Herman, B.M., and Kreidler, T.J. (1974). Martian planetwide crater distributions: Implications for geologic history and surface processes. Icarus 22, 239-263.

Soderblom, L.A., Malin, M.C., Murray, B.C., and Cutts, J.A. (1973). Mariner 9 observations of the surface of Mars in the north polar region. J. Geophys. Res. 78, 4197-4210.

Sutherland, B.P., and Maass, O. (1932). Measurements of the viscosity of gases over a large temperature range. Can. J. Research 6, 428-443.

Sverdrup, H.U. (1937). On the evaporation from the Oceans. J. Marine Res. 1, 3-14.

Tschudin, K. (1946). Rate of vaporization of ice. Helv. Phys. Acta 19, 91-102.

Ward, W.R. (1973). Large scale variations in the obliquity of Mars. Science 181, 260-262.

Yung, Y.L., and Pinto, J.P. (1978). Primitive atmosphere and implications for the formation of channels on Mars. Nature 273, 730-732.

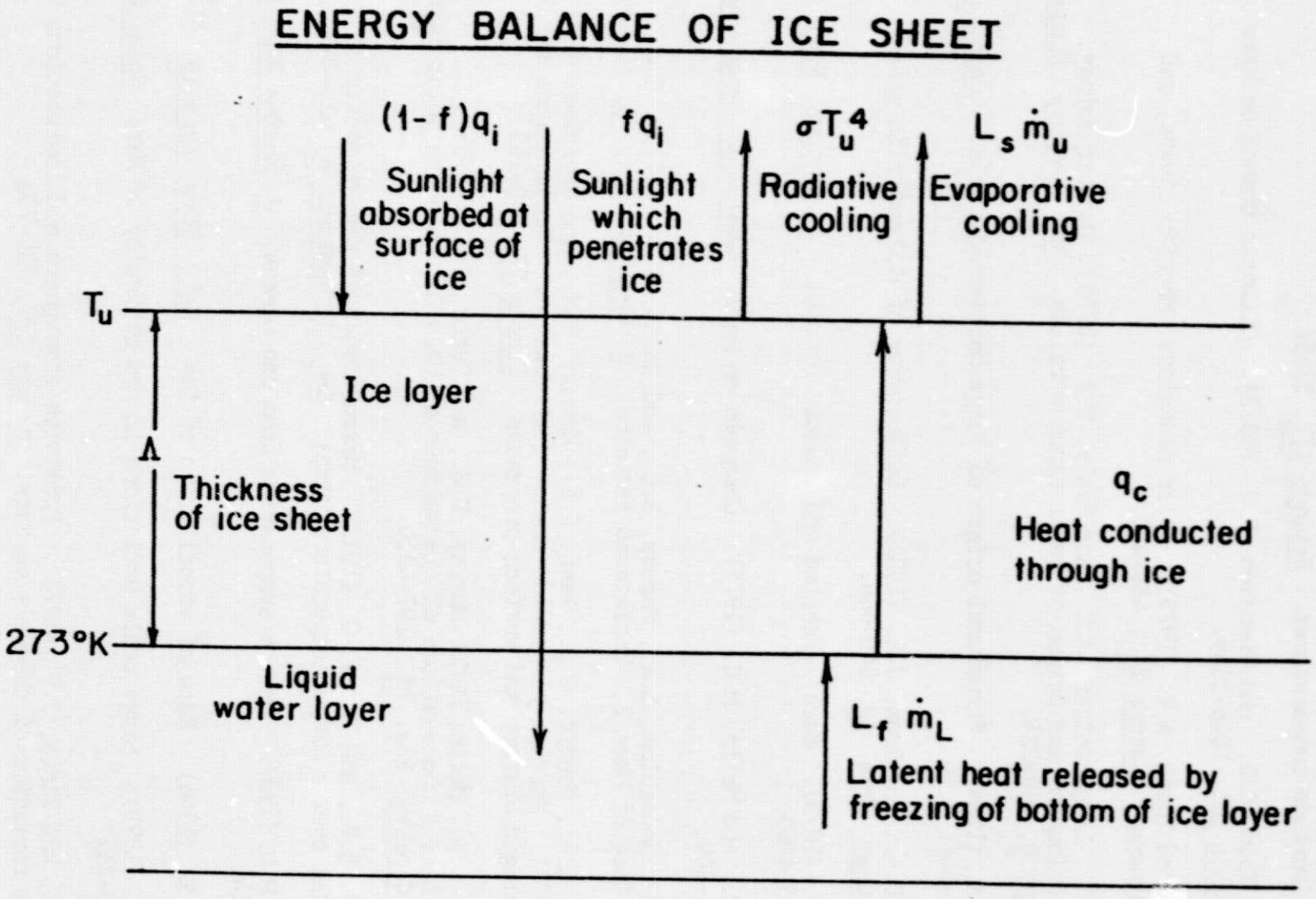

Fig. 1. Schematic diagram of the energy balance for liquid water beneath an illuminated ice sheet.

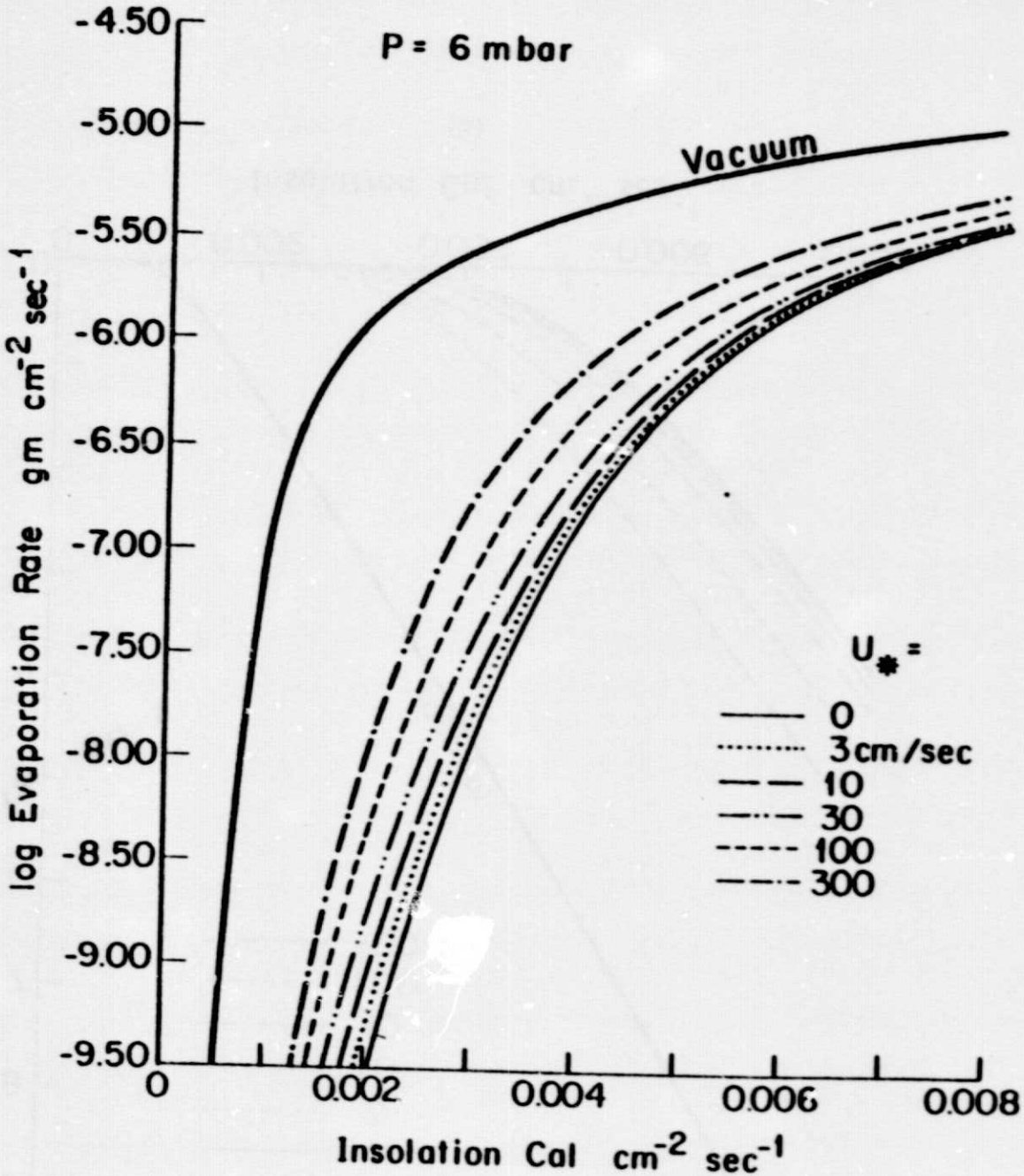

(a)

Fig. 2. Evaporation rate as a function of insolation for 6 mb pressure and for vacuum for various values of the friction velocity. (a): log scale. (b): linear scale

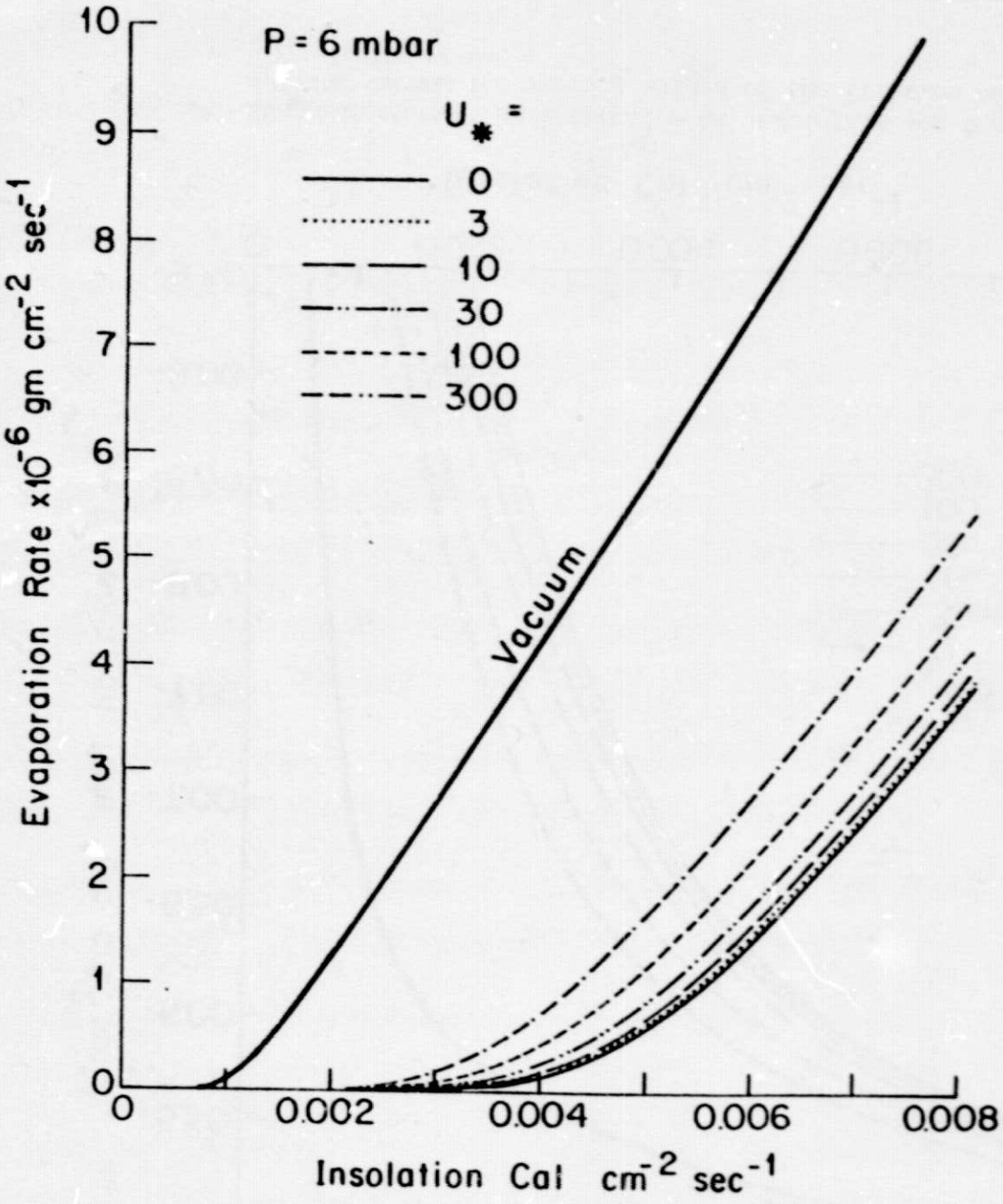
P = 6 mbar
U* =
0
3
10
30
100
300
Vacuum
Evaporation Rate x10^-6 gm cm^-2 sec^-1
Insolation Cal cm^-2 sec^-1
0
1
2
3
4
5
6
7
8
9
10
0
0.002
0.004
0.006
0.008

(b)

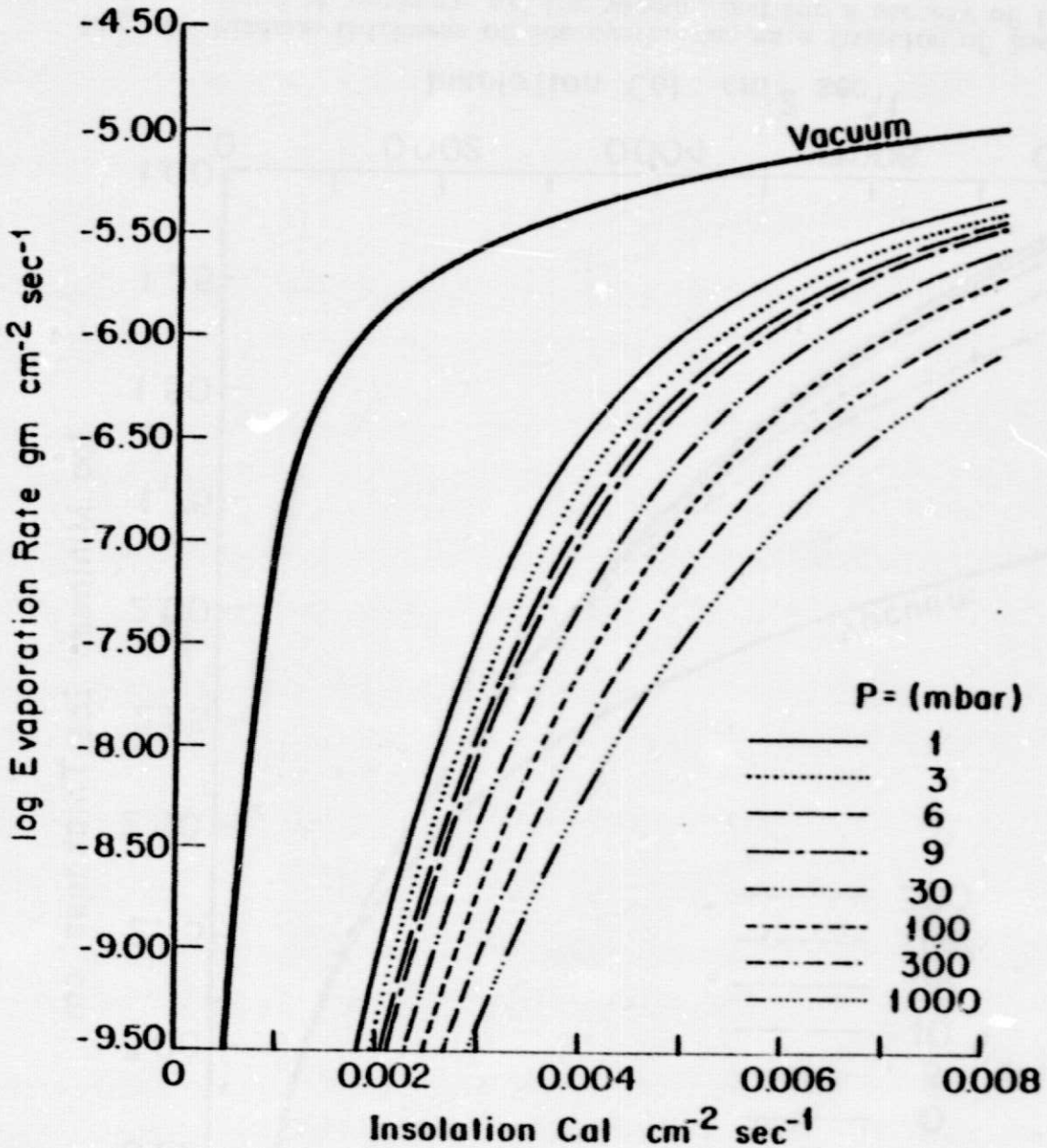

Fig. 3. Evaporation rate as a function of insolation for a variety of pressures for zero friction velocity.

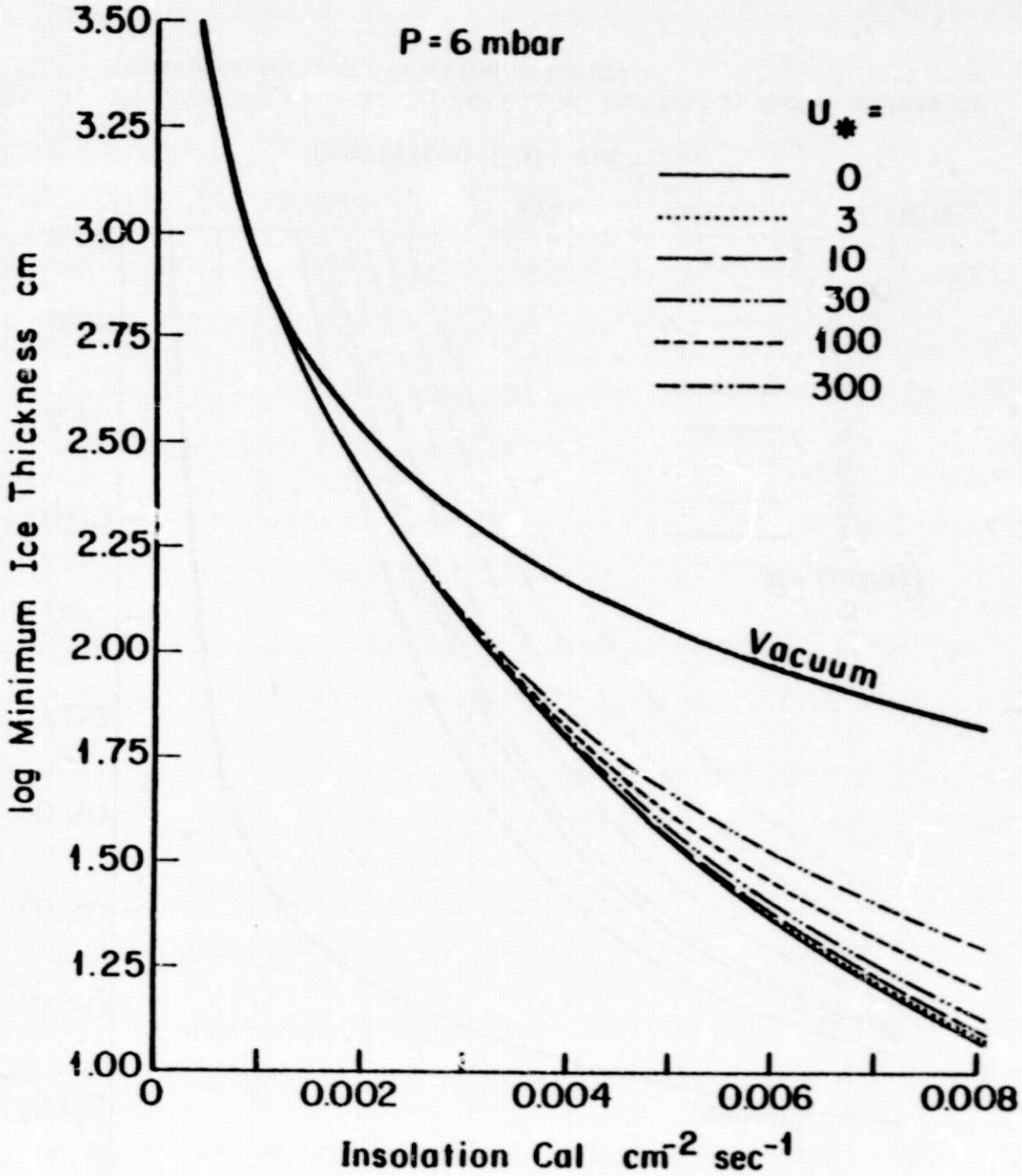

Fig. 4. Minimum thickness of ice overburden as a function of insolation for 6 mb pressure and for vacuum, and for a variety of friction velocities.

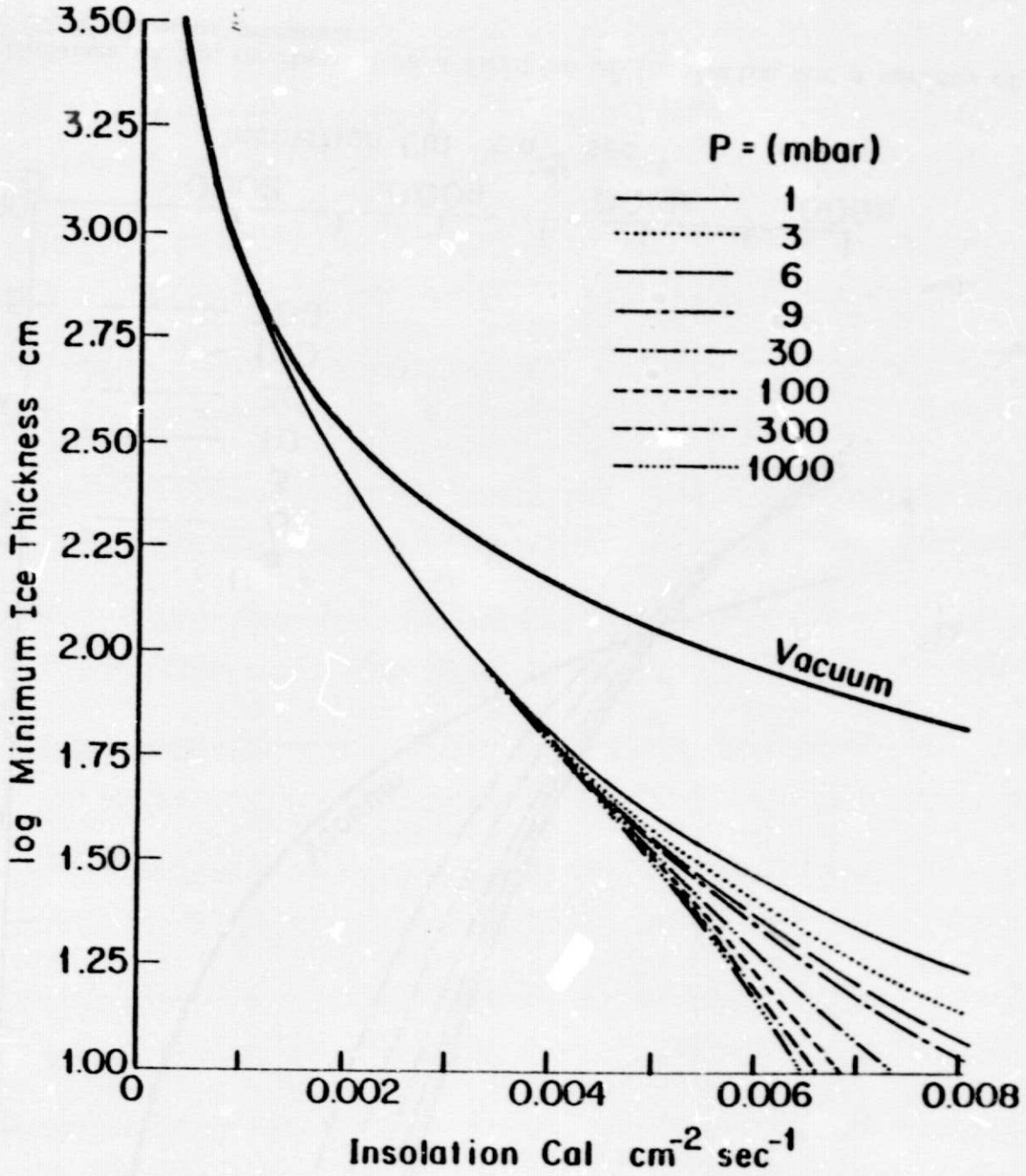

Fig. 5. Minimum thickness of ice overburden as a function of insolation for a variety of pressures and for zero frictional velocity.

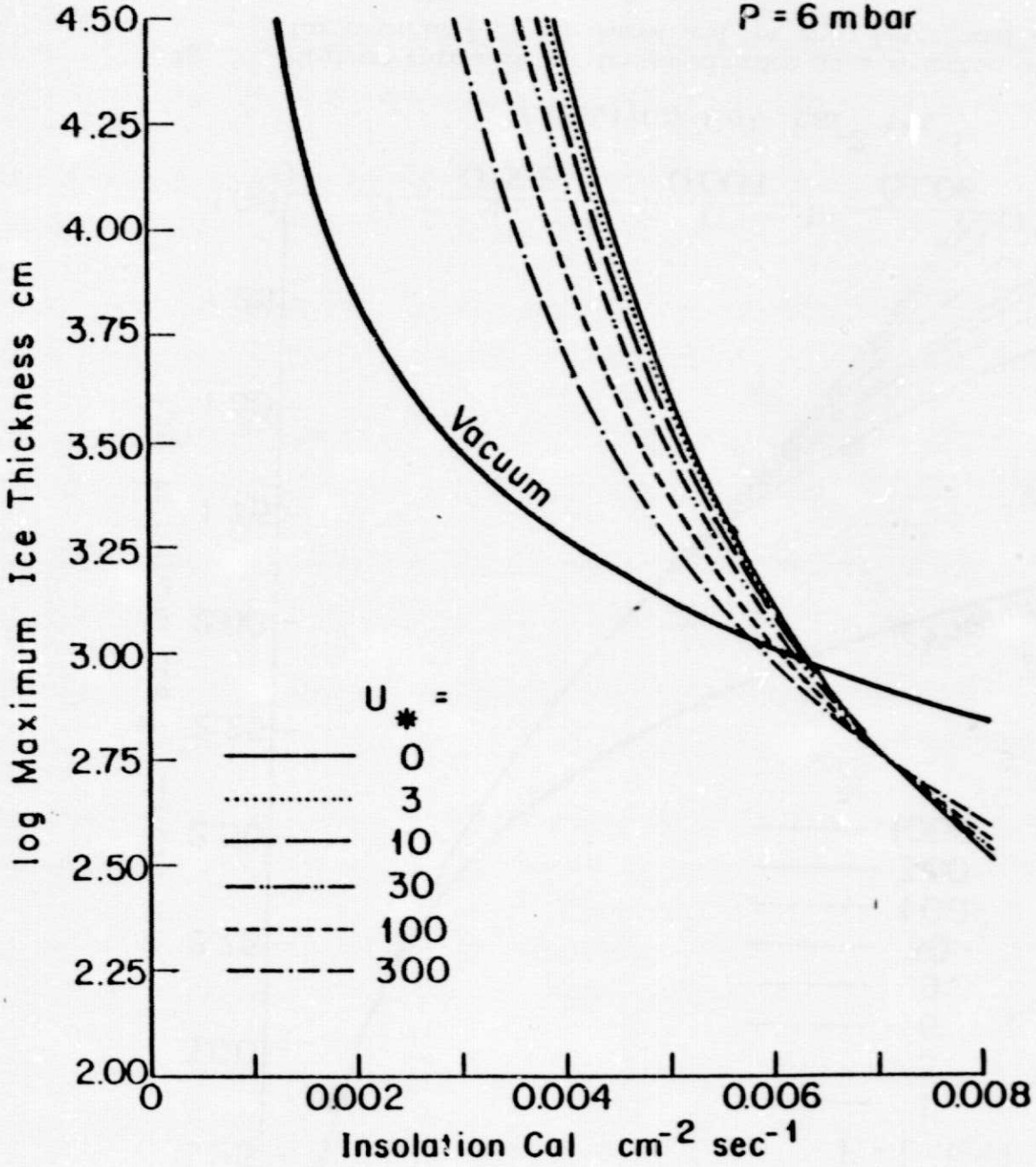

Fig. 6. Maximum thickness of ice overburden as a function of insolation for a variety of frictional velocities and for two choices of pressure.

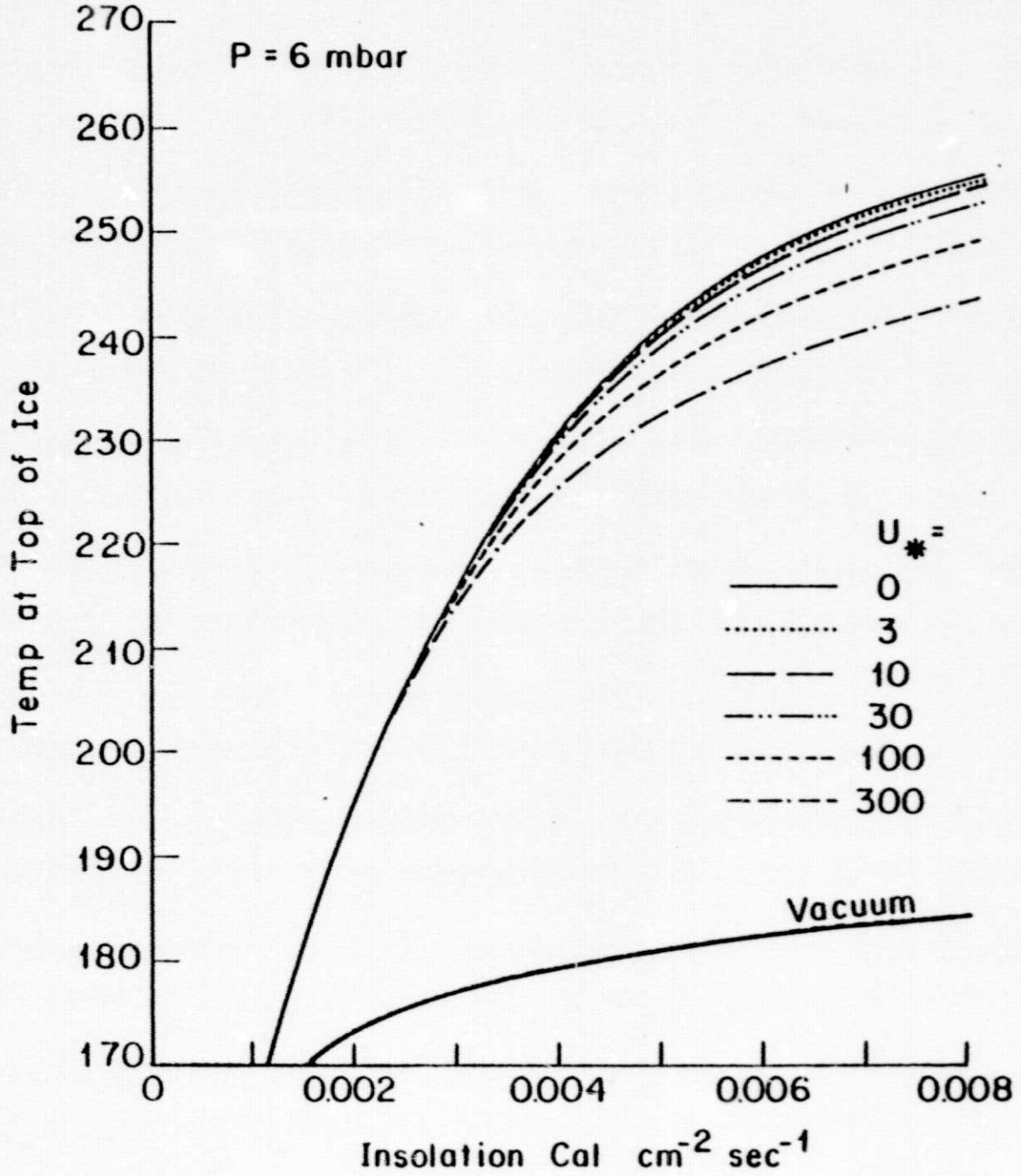

Fig. 7. Equilibrium temperature at the frozen surface of an ice-covered river on Mars as a function of insolation and frictional velocity for two choices of atmospheric pressure.